2. S. V. Fal'kovich, "Propagation of a twisted jet in an infinite space filled with the same fluid," Prikl. Mat. Mekh., 32, No. 1, 282-288 (1967).
3. V. I. Korobko, Theory of Nonsimilitudinous Jets of a Viscous Fluid [in Russian], Saratov Univ. (1977).
4. S. V. Fal'kovich and V. I. Korobko, "Aerodynamics and heat transfer of a twisted jet propagating in an infinite space filled with the same fluid," Izv. Vyssh. Uchebn. Zaved., Mat., No. 7, 87-95 (1969).
5. Z. P. Shul'man, V. I. Korobko, and V. K. Shashmin, "Heat and mass transfer in a submerged axisymmetric nonsimilitudinous jet," Inzh.-Fiz. Zh., 41, No. 4, 645-650 (1981).
6. L. A. Vulis and V. P. Kashkarov, Theory of Jets of Viscous Fluids [in Russian], Nauka, Moscow (1965).
7. G. Beitmen and A. Erdein, Higher Transcendental Functions, Vol. 1, McGraw-Hill.
8. G. N. Abramovich, S. Yu. Krasheninnikov, A. I. Sekundov, and I. P. Smirnova, Turbulent Mixing of Gaseous Jets [in Russian], Nauka, Moscow (1974).
9. V. I. Korobko and S. V. Fal'kovich, "Development of a twisted jet in an infinite space," Izv. Akad. Nauk SSSR, Mekh. Zhidk. Gaza, No. 3, 56-63 (1969).
10. S. Yu. Krasheninnikov, "Study of a submerged air jet with a high rate of twist," Izv. Akad. Nauk SSSR, Mekh. Zhidk. Gaza, No. 6, 148-154 (1971).
11. M. A. Gol'dshtik, Vortices [in Russian], Nauka, Novosibirsk (1981).
12. D. N. Lyakhovskii, "Aerodynamics of twisted jets and its value for flame combustion," in: Theory and Practice of Gas Combustion [in Russian], Gostoptekhizdat, Leningrad (1958), pp. 28-77.

EXPERIMENTAL STUDIES OF A PLANE BUOYANT SURFACE JET

A. N. Shabrin

UDC 532.543

Results are presented from an experimental study of the conditions of formation of a plane buoyant jet with different initial values of the density Froude number.

The need to study buoyant surface jets crises in solving a number of important practical problems such as discharge into special cooler-reservoirs or reservoirs designed for multipurpose use of the heated water from heat and electric power plants, as well as the flow of fresh water into bodies of salt water (estuaries, seas, lakes).

The main feature of fluid flow being examined here is the effect of buoyancy on the propagation of the jet under conditions of stable stratification. The presence of stable stratification creates boundaries between layers of liquid of different densities which are stable with respect to time and space.

The most serious shortcoming of earlier studies of plane buoyant surface jets [1-5] is the absence of steady flow conditions during the experiments, which was due mainly to two factors: the flow of heavy liquid from the working volume via a spillway, and the appearance of a water whirlpool region.

To neutralize the effect of the first factor, the authors of [3] arranged for forced delivery of heavy liquid into the bottom part of the working compartment at a rate exceeding the flow rate of the lighter liquid. This also introduced some distortion into the actual flow pattern, affecting particularly the mixing and entrainment parameters.

A problem involving artificial make-up is complicated, since as much heavy liquid needs to be added to the working compartment as is carried off by the flow of light liquid in the given flow regime. The amount of make-up water can be determined from the relation

---

Institute of Hydromechanics, Academy of Sciences of the Ukrainian SSR, Kiev. Translated from Inzhnerno-Fizicheskii Zhurnal, Vol. 45, No. 1, pp. 42-50, July, 1983. Original article submitted March 12, 1982.

 0022-0841/83/4501-0742$07.50

$$\frac{dq}{dx} = UE. \tag{1}$$

However, the main difficulty is that the entrainment (the coefficient E) is not known beforehand. In most cases it is the flow characteristic being studied.

Mixing and entrainment processes in the propagation of a jet into a reservoir depend on many factors, including on waves on the free surface in the vicinity of the discharge of the jet. The conditions of the appearance of such waves are characterized by the Froude number [6] of the flow entering the reservoir:

$$\mathrm{Fr}_0 = U_0/\sqrt{gH_0}. \tag{2}$$

When $\mathrm{Fr}_0 < 1$, the free surface will be undisturbed. When $\mathrm{Fr}_0 > 1$, waves will be formed on the free surface. The conditions of inflow of the jet in [3] were such that the Fr_0 number was greater than 1.0 in several cases.

The methodology of the earlier studies did not include investigation of jets of uniform-density liquids under the same laboratory conditions and with the same basic flow parameters as in the study of buoyant jets. Thus, data for other types of flows [7] was used in certain cases [3] to compare results.

The present work attempts to experimentally study the conditions of formation of a buoyant surface jet, excluding the effect of such factors as forced makeup and whirlpool flow.

In studying buoyant surface jets it is necessary to consider the conditions under which a layer of heavy liquid (salt or cold water) may be present or absent in the bottom region at the outfall section of the discharge channel, this being the same liquid that fills the reservoir. These conditions are determined by the density Froude number [8]

$$\mathrm{Fr}_0' = U_0 \Big/ \sqrt{g\,\frac{\Delta\rho}{\rho_f}\,H_0}. \tag{3}$$

When $\mathrm{Fr}_0' < 1$, such a bottom layer of salt or cold water is present in the discharge channel. When $\mathrm{Fr}_0' > 1$, it is absent.

The conditions of discharge of a plane buoyant surface jet, the results of which are presented below, were characterized by the following values of the conventional and density Froude numbers: $\mathrm{Fr}_0 < 1$, $\mathrm{Fr}_0' > 1$, and by the Reynolds numbers $9\cdot10^2 \leqslant \mathrm{Re}_R = \frac{U_0 R_0}{\nu} \leqslant 4\cdot10^3$.

The studies were conducted on a laboratory unit, the basic setup of which is shown in Fig. 1. The walls and bottom of the delivery channel, working compartment, and salt-water reservoir were made of glass. The distributors 4 and 11 were made of polyvinyl chloride tubes. The main parts of the unit and their dimensions were as follows: the length of the channel 6 was 80 cm, its width was 12 cm; the working compartment 7 measured 250 and 12 cm, respectively; the distance between the level of the channel bottom and the working compartment was 17 cm; the salt-water reservoir 10 was 380 cm long and 200 cm wide; the fresh water tank 1 was of 25 m^3 capacity, while the salt-water tank 13 was of 1.1 m^3 capacity. The initial relative difference in densities used in the tests ranged within $0.0105 \leqslant \Delta\rho/\rho_f = (\rho_c - \rho_f)/\rho_f \leqslant 0.0120$.

The test method included the following sequence of operations: a prepared solution of salt water of the necessary concentration was moved from the tank 13 by means of the pump 12 through the distributor 11 into the reservoir 10 and filled the latter to the level of the channel bottom 6. After the liquid in the reservoir 10 became still, pump 2 was turned on and fresh water from the container 1 was pumped into the constant-head tank 3. Flow rate was measured at the outlet of this tank. The fresh water from the tank 3 was delivered to the reservoir 5, from which it moved by gravity into the reservoir 6 and the working compartment 7. The fresh water then fell freely from the compartment 7 into the salt-water reservoir 10. Salt water was continually added to the reservoir 10 during the experiments so as to ensure a nearly constant level of salt water in this reservoir — a level differing negligibly from the level of the free surface of the water in the reservoir. The elevation of the top of the spillway 9 was established in accordance with the prescribed depth of water at the mouth of the channel 6 for the appropriate flow rate. The freshened surface layer from the reservoir 10 was discharged over the spillway 9 into the section 14, where the mixed water

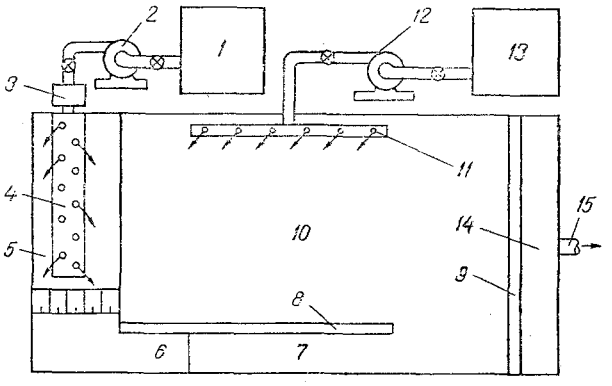

Fig. 1. Basic diagram of the experimental unit: 1) fresh-water reservoir, W = 25 m^3; 2) pump; 3) constant-head tank with meter; 4, 11) distributors; 5) fresh-water reservoir; 6) channel; 7) working compartment; 8) dividing wall; 9) spillway; 10) salt-water reservoir; 12) pump; 13) salt-water tank; 14) discharge section; 15) discharge pipe.

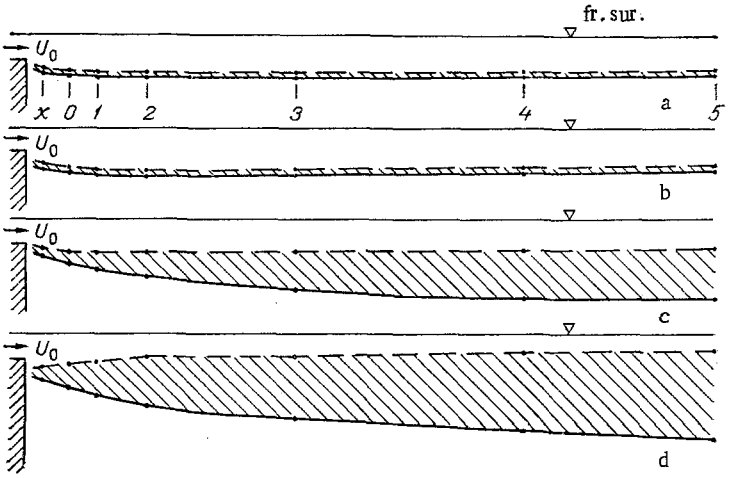

Fig. 2. Dividing layer of liquids with different densities: x-5) sections at which the density profiles *a*, b, c, d, equal, respectively, to $Fr_0' =$ 1.02, 1.32, 2.54, and 4.14, were measured.

was then sent along a pipe 15 and removed from the system. Since the flow was now stabilized on the average, we proceeded directly to measurement of the density and velocity characteristics.

Steady flow was ensured during the tests as a result of the following features of the unit design and test method. The dividing wall 8 had a slit 15 mm wide at the bottom which freely connected the compartment 7 with the reservoir 10 along the entire length of the working section and ensured natural makeup of the salt water in the working compartment. The free flow of the fresh-water jet from the working compartment into the reservoir 10 ensured the free spreading of a thin layer of fresh water over the entire surface of the reservoir filled with salt water, i.e., the fresh water did not encounter any artificial barriers as it left the working compartment. There was thus no whirlpool region to distort the general flow pattern.

The velocity structure of the flow was studied by visual observation. We used finely dispersed aluminum powder as an indicator. Each point on the velocity profile was obtained from the statistical analysis of 100 or more instantaneous values of velocity. The sections at which the velocity profiles were measured were located at distances from the mouth $x/H_0 =$ 0, 10.3, 28.7, 53.5, and 73.5.

TABLE 1. Initial Flow Parameters and Thickness of the Dividing Layer

No. of test	U_0	H_0	$\left(\frac{\Delta\rho}{\rho_f}\right)_0$	Fr_0'	$(Re_0)_R$	Ri_0	Thickness of dividing layer at sections			
							2	3	4	5
1	5,15	2,50	0,0105	1,02	910	0,970	0,65	0,50	0,50	0,50
2	6,70	2,50	0,0105	1,32	1180	0,575	0,90	0,75	0,75	0,75
3	13,50	2,50	0,0115	2,54	2340	0,155	2,1	4,0	4,3	4,4
4	22,40	2,50	0,0120	4,14	3950	0,059	4,4	5,9	7,0	8,3

The studies were conducted at different flow rates, but the water depth at the mouth section of the channel 6 was kept constant (H_0 = 2.5 cm) by means of the spillway 9. The density profiles were found by means of a platinum transducer which measured the electrical conductivity of the medium. The transducer was calibrated before and after the tests. The sections at which the density profiles were measured were located at distances from the mouth x/H_0 = 2.2, 4.9, 8.0, 12.8, 28.7, 53.5, and 73.5. The sensitivity of the recording apparatus was such that we were able to determine the minimum value of salinity to within 0.1 of the maximum value.

The test data included measurement of characteristic flow parameters at the channel outlet. Analysis of this data [9] showed that the fresh-water flow at the channel mouth had all of the characteristics of boundary-layer flow under open-flow conditions.

It should be noted that, in contrast to classical jet flows [10], when a mixing layer characterized by a constant initial velocity U_0 along the flow axis begins immediately after the mouth section ($x/H_0 > 0$), in our case the flow in this region is formed by another flow with a developed velocity profile typical of open channels, and the mixing layer as such is absent.

The interaction of the fresh jet with the salt water filling the reservoir forms a dividing layer with a variable density, its density increasing with depth under conditions of stable stratification. The dividing layer has two boundaries: upper and lower. It can be seen from Fig. 2 that the development of this dividing layer depends significantly on the initial flow conditions — specifically, on the kinetic energy of the fresh-water flow entering the salt-water reservoir and on the relative difference of the densities of the interacting liquids. The tests, the results of which are shown in graphical form in Fig. 2, can be divided into two groups: group I — tests Nos. 1, 2; group II — tests Nos. 3, 4. The distinctive feature of the tests of the first group is that the dividing layer, having formed directly after the mouth, undergoes little change in its transverse dimensions — the top and bottom boundaries of the layer are nearly parallel as they move in the depth direction, if we do not consider a certain slight expansion in the initial sections followed by a contraction and subsequent stabilization. It is interesting to note that in both tests the dividing layer at first begins to descend. It then gradually surfaces and its position becomes stable. The difference between the layers in the tests is defined by quantitative estimates: in test No. 1 (Fr_0' = 1.02), descent of the layer ends at a distance of about 12 cm from the mouth, while the submersion stage is completed in test No. 2 (Fr_0' = 1.32) at a distance of about 32 cm. The same situation prevails with the thicknesses of the layers h_{la}, numerical values of which are shown in Table 1. The graph of the change in density within the layer is a linear function of depth (see Figs. 3a, b, $\Delta/\Delta_m = (\Delta\rho/\rho_f)/(\Delta\rho/\rho_f)_{max} = f_1[y/(\delta_1/2)_s]$), which is typical of all of the density profiles measured at sections x-5. The density gradient is lower, the greater the number Fr_0'.

The results of the group II tests are both similar to and different from the group I tests. First of all, the formation of the dividing layer is significantly affected by the fresh-water flow, not only in the immediate vicinity of the mouth but also far from the latter. The rate of increase in the thickness of the dividing layer and the distance from the mouth at which this increase occurs are directly dependent on the value of Fr_0'. Secondly, the dividing layer is subdivided into two sublayers (Figs. 3c, d) with different density gradients — the upper sublayer has a lower density gradient than the lower sublayer. The division into sublayers does not occur immediately after the mouth, but rather a certain distance from it: $x \simeq (16\text{-}20)H_0$.

Analysis of the empirical data obtained allowed us to establish that the density gradient in the dividing layer decreases, with an increase in Fr_0' and increasing distance from the

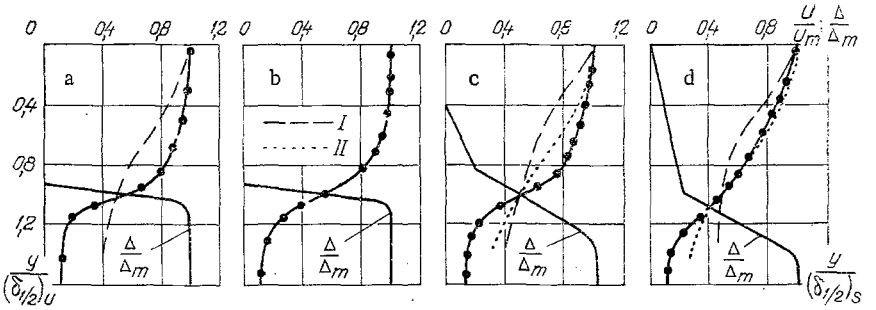

Fig. 3. Distribution of relative density difference in the dividing layer and mean velocities through the depth of the flow at $x/H_0 = 73.5$: a, b, c, d) $Fr_0' = 1.02, 1.32, 2.54, 4.14$; I) uniform jet; II) from Eq. (5).

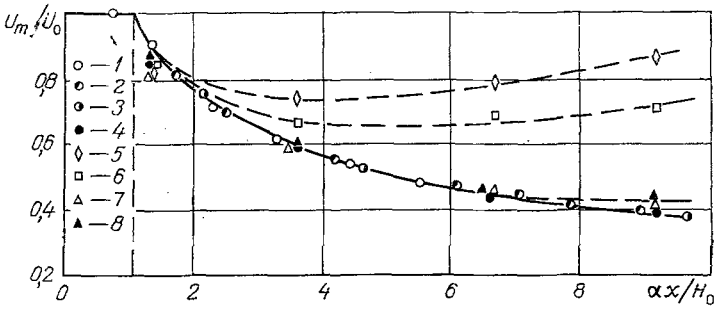

Fig. 4. Change in velocity along the axis of a plane jet as well as along the free surface for a uniform liquid and under conditions of stable stratification: 1) data of Fertman ($\alpha = 0.11$); 2) Turkus ($\alpha = 0.09$); 3) Proskur ($\alpha = 0.12$) [1)-3) were taken from [11]]; 4) plane jet with a free surface ($\alpha = 0.125$) [9]; 5) $Fr_0' = 1.02$; 6) 1.32; 7) 2.54; 8) 4.14.

mouth section, to a certain limiting value. After the density gradient reaches this value, the top boundary of the dividing layer begins to break down, and this is accompanied by the removal of the liquid into the top part of the jet flow. The intensity of this process is greater than the intensity of the similar phenomenon occurring at the lower boundary of the dividing layer and the associated makeup of salt water from lower-lying layers. This difference in intensity leads to separation of the dividing layer into two sublayers with different density gradients. This structure is unstable — it is transformed continuously along with the velocity field of the flow. Since the dividing layer is a component part of the jet flow being studied, an increase in its transverse dimensions is accompanied by a decrease in the mean velocity of the flow and, thus, in the energy of the vortices breaking up the upper boundary of the dividing layer and allowing makeup of the salt water of the dividing layer from lower-lying layers. As a result, the gradient of the lower sublayer stabilizes, while the upper sublayer gradually degenerates. Complete stabilization of the flow begins when the dividing layer again acquires a single density gradient, corresponding to the kinetic energy of the flow at the given section. Here it should be noted that the removal of salt water from the bottom layer causes the density of the liquid in the top jet layer to increase and the relative difference between the densities of the stratified liquids to decrease. However, since the kinetic energy of the flow decreases more rapidly, this development does not affect the stability of the dividing layer.

The similarity between the results of the tests in groups I and II consists of the linearity of the density profile, regardless of whether or not the dividing layer is subdivided into two sublayers.

We will begin our analysis of the velocity structure of the flow with results (see Fig. 4) characterizing the change in the mean velocity along the free surface with different values of the initial numbers Fr_0'. For comparison, the same figure shows data for a uniform surface

jet [9] and a plane-parallel jet [11]. It can be seen from the figure that the test data obtained for uniform liquids agree well with each other and with the theoretical relation

$$\frac{U_m}{U_0} = \frac{1.2}{\sqrt{\alpha \frac{x}{H_0} + 0.41}}. \quad (4)$$

As concerns the data on the buoyant jet, a certain degree of agreement is seen here. However, while the test points agree with Eq. (4) in the range $0 \leqslant \alpha x/H_0 \leqslant 7$ for tests with numbers $Fr_0' = 2.54$ and 4.14, agreement is limited to the range $0 \leqslant \alpha x/H_0 \leqslant 1.5-2.0$ for tests with the numbers $Fr_0' = 1.02$ and 1.32. The curves subsequently deviate sharply from the generalized relation (4), and the ratio U_m/U_0 tends to increase — evidence of acceleration of the flow at a certain distance from the mouth. This phenomenon is evidently connected mainly with a decrease in the turbulence level of the flow and resistance. This process is not as noticeable in tests with significant Fr_0' numbers, at least within the working section where the measurements were made.

Figure 3 shows mean velocity profiles of the buoyant jet in the coordinates $U/U_m = f[y/(\delta_{1/2})_U]$. They all pertain to one section $x/H_0 = 73.5$ and characterize the flow at different Fr_0' numbers. For comparison, Figs. 3a, c, d show (with dashed lines) velocity profiles obtained in studying the uniform surface jet at the same sections and with roughly (to within 5-10%) the same velocities U_0 at the mouth of the delivery channel. It can be seen from the figure that the mean velocity profiles for the uniform surface jet and buoyant jet differ considerably. This difference is greater, meanwhile, the lower the value of Fr_0'. At $Fr_0' = 1.02$, 1.32, and 2.54, the mean velocity profiles in the range $0 < y/\delta_{1/2} \leqslant 1.1$ are qualitatively similar to the velocity profiles typical of liquid boundary-layer flows.

The dashed lines in Figs. 3c, d show profiles corresponding to an equation of the type [12]

$$\frac{U}{U_m} = \left[1 + 0.41\left(\frac{y}{\delta_{1/2}}\right)^2\right]^{-2}, \quad (5)$$

which satisfactorily describes the experiment at $Fr_0' = 4.14$ and does not fully agree with the test data at lower values of Fr_0'.

Based on analysis of the experimental data obtained here, it can be concluded that in the propagation of a plane buoyant surface jet close to or far from the mouth section, the transformation of the mean velocity field ends in a manner similar to that depicted in Figs. 3a-c, regardless of the initial number Fr_0'.

NOTATION

x, y, cartesian coordinate axes; the 0x axis is directed along the mean-velocity vector on the free surface; the 0y axis is normal to the 0x axis and directed downward; U, V, components of mean flow velocity in the 0x and 0y directions, cm/sec; q, unit flow rate of the liquid, cm^2/sec; E, entrainment coefficient; U_0, mean flow velocity in the 0x direction at the mouth section, cm/sec; H_0, total flow depth at the mouth section, cm; ρ_c, ρ_f, density of salt and fresh water, respectively; R_0, hydraulic radius of flow at the mouth section, cm; ν, kinematic viscosity, cm^2/sec; U_{max}, mean flow velocity at the free surface, cm/sec; $(\delta_{1/2})_U$, distance from free surface to the point where $U = \frac{1}{2} U_{max}$; $(\delta_{1/2})_s$, distance from the free surface to the point where $\frac{\Delta\rho}{\rho_n} = \frac{1}{2}\left(\frac{\Delta\rho}{\rho_f}\right)_{max}$; Ri_0, Richardson number.

LITERATURE CITED

1. K. Ya. Kind, "Study of surface flows," Tr. Koord. Soveshch. Gidrotekh., 11, 129-141 (1964).
2. I. A. Sherenkov and A. P. Netyukhailo, "Hydraulic calculation of flow movement in a reservoir," Tr. Vses. Nauchno-Issled. Inst. Vodosnabzh. Kanaliz. Gidrotekh. Sooruzh. Inzh. Gidrogeol., 11, 5-40 (1968).
3. V. H. Chu and M. R. Vanvari, "Experimental study of turbulent stratified shearing flow," J. Hydraulics Division, Proc. Am. Soc. Civ. Eng., 102, No. HY6, 691-706 (1976).

4. T. H. Ellison and J. S. Turner, "Turbulent entrainment in stratified flows," J. Fluid Mech., 6, 423-448 (1959).
5. H. Stefan, "Stratification of flow from channel into deep lake," J. Hydraulics Division, Proc. Am. Soc. Civ. Eng., 96, No. HY7, 1417-1433 (1970).
6. I. I. Agroskin, G. T. Dmitriev, and F. I. Pikalov, Hydraulics [in Russian], Énergiya, Moscow-Leningrad (1964).
7. W. N. Schwarz and W. P. Cozart, "The two dimensional wall jet," J. Fluid Mech., 10, 481-495 (1961).
8. Hydrodynamics of Coastal Areas and Estuaries [in Russian], Gidrometeoizdat, Leningrad (1970).
9. A. N. Shabrin, "Plane jet in a reservoir with a free surface," in: Hydraulics and Hydraulic Engineering, Vol. 32, Tekhnika, Kiev (1981), pp. 64-70.
10. A. A. Townsend, Structure of a Turbulent Flow with Transverse Shear [Russian translation], IL, Moscow (1959).
11. G. N. Abramovich, Theory of Turbulent Jets [in Russian], Fizmatgiz, Moscow (1960).
12. P. B. B. Lal and N. Rajaratham, "Experimental study of bluff buoyant turbulent surface jets," J. Hydraul. Res., 15, No. 3, 261-275 (1977).

FEASIBILITY OF PRODUCING PRESCRIBED DISTRIBUTION OF TEMPERATURE GRADIENT WITH ARRAY OF SUBMERGED JETS

S. A. Fedyushin, V. N. Papkovich, and Yu. A. Milevich

UDC 532.525.2

It is demonstrated that it is feasible to produce a region with a linear transverse temperature profile with the necessary temperature gradient along the jet height.

Considerable interest of researchers has been attracted to the feasibility of producing rather large transverse density gradients by means of devices utilizing submerged jets with intricate initial and velocity profiles [1-5].

The results of several studies [6, 7] suggest that using the method of the equivalent problem in theory of heat conduction is expedient even in the design of non-self-adjoint turbulent liquid or gas jets.

We will write the equations of a turbulent boundary layer as

$$\rho U\frac{\partial U}{\partial t}+\rho U\frac{\partial U}{\partial y}=\frac{\partial}{\partial y}\tau_{\text{т}},\quad \frac{\partial}{\partial z}(\rho U)+\frac{\partial}{\partial y}(\rho U)=0,$$
$$\rho U c_p\frac{\partial}{\partial z}\Delta T+\rho U c_p\frac{\partial}{\partial y}\Delta T=\frac{\partial}{\partial y}q_{\text{т}},\quad \Delta T=T-T_0. \tag{1}$$

The change of variables

$$\xi=\xi(x,\ y);\quad \eta=\eta(x,\ y);\quad \xi_{\text{т}}=\xi_{\text{т}}(z,\ y);\quad \eta_{\text{т}}=\eta_{\text{т}}(z,\ y) \tag{2}$$

reduces system (1) to the system of linear equations

$$\frac{\partial}{\partial\xi}(\rho U^2)=\frac{\partial^2}{\partial\eta^2}(\rho U^2);$$
$$\frac{\partial}{\partial\xi_{\text{т}}}(\rho U c_p\Delta T)=\frac{\partial^2}{\partial\eta_{\text{т}}^2}(\rho c_p U\Delta T). \tag{3}$$

A solution of the equations of a boundary layer for jet-type sources by the method of an

Belorussian Polytechnic Institute, Minsk. Translated from Inzhenerno-Fizicheskii Zhurnal, Vol. 45, No. 1, pp. 50-53, July, 1983. Original article submitted February 26, 1982.

 0022-0841/83/4501- 0748$07.50